Research Journal of Applied Sciences, Engineering and Technology 4(24): 5578-5585, 2012
ISSN: 2040-7467

Submitted: April 27, 2012 Accepted: May 18, 2012 Published: December 15, 2012

Fanno Flow in Microchannels

[1,4]M.A. Al-Nimr, [2]V.A. Hammoudeh, [2]M.A. Hamdan and [3]M.H. Es-Saheb
[1]Mechanical Engineering Department, Jordan University of Science and Technology, Irbid, Jordan
[2]Mechanical Engineering Department, University of Jordan, Amman 11942, Jordan
[3]Mechanical Engineering Department, King Saud University, Riyadh 11421, Saudi Arabia
[4]Royal Scientific Society, Amman-Jordan

Abstract: In this study, the Fanno flow problem has been theoretically investigated using both, first order and second order velocity-slip boundary conditions models and then compared to the no-slip boundary conditions solution. The objective is to study the behavior of the flow predicted by the two slip models. Then, an attempt will be made to establish criteria for using the no-slip and the two velocity-slip models. The Fanno flow is an ideal gas adiabatic flow in constant area duct with friction. It is found that the velocity profile for the two velocity-slip models has the same shape as the no-slip model velocity profile but with an amount of slip at the wall which increases as the *Knudsen number*, *Kn*, increases. Also the effect of the slip has on the compressible flow characteristics have been examined. It shows that as the *Kn* increases, the skin friction coefficient C_f and the Darcy friction coefficient *f* decrease. Overall, it is concluded that for an adiabatic compressible flow in circular microchannel, for $Kn \leq 0.01$ there is no need to apply any velocity-slip model as the no-slip model gives sufficiently accurate predictions. As for the range $0.01 \leq Kn \leq 0.1$, the first order velocity slip model should be applied and so for this range, there is no necessity to use the second order velocity-slip model.

Keywords: Fanno flow, microchannels, navier-stokes equations, velocity-slip model, compressible flow

INTRODUCTION

In the recent years the industry, driven by the constant quest for miniaturization of gadgets and machines, has developed a number of manufacturing processes that can create extremely small electronic and mechanical components. This has led to the increase of interest in the micro-scale fluid and heat transfer research. It was observed that in such small devices the fluid flows differ from those in macroscopic machines and cannot always be predicted from conventional flow models such as the Navier-Stokes equations with no-slip boundary condition at a fluid-solid interface. Slip flow, thermal creep, rarefaction, viscous dissipation, compressibility, intermolecular forces and other unconventional effects may have to be taken into account. Recently, Matsuda *et al*. (2011) studied pressure-sensitive molecular film for micro gas flows. Also, Demsis *et al*. (2009) and Marino (2009) worked on experimental determination of heat transfer coefficient in the slip regime and its anomalously low value, as well as experiments on rarefied gas flows through tubes. Meanwhile, earlier works by Morini *et al*. (2006) on experimental investigations on friction characteristics of compressible gas flows in microtubes is reported. Later, experimental investigations are published by Celata *et al*. (2007) and Gamrat *et al*. (2008) on compressible flow in microtubes and modeling of roughness effects on laminar flow in microchannels.

For gases, micro-fluid mechanics has been studied by incorporating slip boundary conditions, thermal creep, viscous dissipation as well as compressibility effects into the continuum equations of motion, but it has a number of limitations. Some of these limitations are reported in the works of many investigators such like: the studies of Hsieh *et al*. (2004) on Gas flow in a long microchannel; Morini *et al*. (2006) on friction characteristics of compressible gas flows in microtubes; Kim and Kim (2007) on closed-form correlations for thermal optimization of microchannels; Morini *et al*. (2007) on experimental analysis of pressure drop and laminar to turbulent transition for gas flows in smooth microtubes; Cai and Boyd (2007) on compressible gas flow inside a two-dimensional uniform microchannel; Colin *et al*. (2010) work on validation of a second-order slip flow model in rectangular microchannels; Araki *et al*. (2010) on experimental investigation of gaseous flow characteristics in microchannels; and Kashid *et al*. (2011) on mixing efficiency and energy consumption for five

Corresponding Author: M.A. Al-Nimr, Mechanical Engineering Department, Jordan University of Science and Technology, Irbid, Jordan

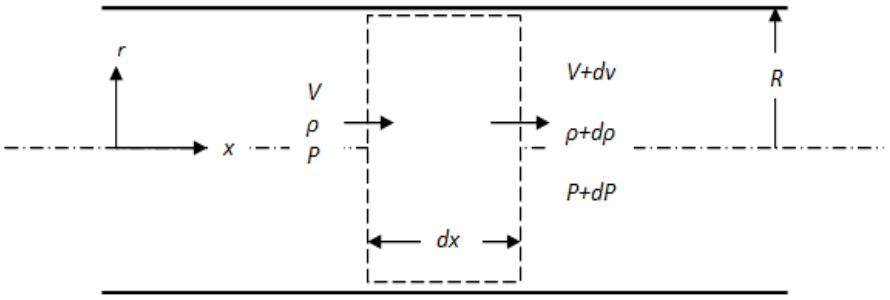

Fig. 1: Schematic diagram of the problem

generic microchannel designs. Molecular-based models have also been attempted for certain ranges of the operating parameters by Matsuda *et al.* (2011, 2009).

Since the continuum model is mathematically easier to handle than alternative molecular models it should be used as long as it is applicable. Thus, careful examination of the validity of the Navier-Stokes equations is very important. In order to be able to solve the Navier-Stokes equations for any flow situation a number of initial and boundary conditions need to be applied. Here the *Knudsen number* definition has to be introduced as the ratio between the mean free path (λ) and the characteristic Length (L) and is generally the most important parameter determining the flow regime. The different Knudsen number regimes are determined empirically and are therefore only approximate for particular flow geometry. Traditionally, the no-slip boundary condition at a fluid-solid interface is enforced in the momentum equation and an analogous no-temperature-jump condition is applied in the energy equation. In practice, the no-slip/no-jump condition leads to fairly accurate predictions as long as Kn<0.001. Beyond that, the equilibrium does not hold and a certain degree of tangential velocity slip and temperature jump must be allowed. This is the case with the microchannel flow so for it the appropriate velocity-slip/temperature-jump boundary condition should be used. First-order velocity-slip/temperature-jump boundary conditions are generally applicable to the Navier-Stokes equation in the range between 0.001<Kn<0.1. The transition region occupies the range between 0.1<Kn<10 and second-order or higher slip/temperature-jump boundary conditions are applicable there along with some molecular-based models.

In the last few years, the increased interest in the micro-flow area research has resulted in a large number of theoretical and experimental publications on the subject by John (1984), White (1991), Choi *et al*. (1991), Harley *et al*. (1995), Choquette *et al*. (1996), Ho and Tai (1998), Karniadakis and Beskok (2002), Chuang *et al*. (2003), Koochesfahani and Nocera (2007), Yang *et al*. (2010), Pitakarnnop *et al*. (2010) and Petropoulos *et al*. (2010). Gad-el-Hak (1999, 2002) has published a couple of reviews and recently Morini *et al*. (2011), which serve as an excellent introduction into the micro-flow area of research. However, due to the variety of problems and approaches there are still a number of problems that have not been addressed as reported by Wu and Cheng (2003), Petropoulos *et al*. (2010) and Kim *et al*. (2010). The scope of the present study is to investigate the effect of implementing the velocity-slip boundary conditions on the case of the adiabatic flow in a constant-area duct with friction, also known as Fanno flow. The classical Fanno flow case with the no-slip boundary conditions is standard issue in most of the fluid dynamics textbooks, White (1991) and John (1984), but up to our knowledge it has not been investigated using any of the velocity-slip models so far. The objective of the present study so, is to investigate the effect of both the first order and the second order slip models on the hydrodynamic behavior of compressible flow in microchannels. This aims to establish criteria that justify the use of the first order slip model instead of the second order slip model.

MATHEMATICAL FORMULATION

In order to derive a relation for a compressible flow in microchannel, the control volume shown in Fig. 1 is considered. When the momentum equation is applied to the differential element shown the resulting equation is:

$$-Adp-\tau_f(dx)\frac{4A}{D}=\rho AVdV \qquad (1)$$

where, τ_f is the shear stress due to the wall friction and D is the pipe diameter. By introducing the friction factor $f = 4\ \tau_f\ /\ (1/2\rho V^2)$ and the Mach number definition ($V = M\sqrt{\gamma RT}$) is introduced and then the whole equation divided by p, this can be rewritten as:

$$dp+\frac{1}{2}\gamma M^2 f\frac{dx}{D}+\gamma M^2\frac{dV}{V}=0 \qquad (2)$$

Now in order to obtain an expression for the Mach number M in terms of distance x, the dp/p and dV/V terms

must be replaced. For that, first the ideal-gas equation of state ($\rho = p/RT$) is used, the logarithm is taken and differentiated resulting in the following equation:

$$\frac{dp}{p} = -\frac{dM}{M} + \frac{1}{2}\frac{dT}{T} = 0 \tag{3}$$

In the same manner, using the above mentioned Mach number definition ($V = M\sqrt{\gamma RT}$), taking the logarithm an then differentiating results:

$$\frac{dV}{V} = \frac{dM}{M} + \frac{1}{2}\frac{dT}{T} \tag{4}$$

Since the flow into consideration is adiabatic, the stagnation temperature $T_0 = T(1+ \gamma - 1/2M^2)$s constant, so if the definition is used as above it will result:

$$\frac{dT}{T} + \frac{d\left(1+\frac{\gamma-1}{2}M^2\right)}{1+\frac{\gamma-1}{2}M^2} = 0 \tag{5}$$

After combining the Eq. (2), (3), (4) and (5) and a lengthy procedure of rearrangement and integration[10] the following equation is obtained:

$$\frac{fL_{\max}}{D} = \left(\frac{\gamma+1}{2\gamma}\right)\ln\left(\frac{(\gamma+1)M^2}{2\left(1+\frac{\gamma-1}{2}M^2\right)}\right) + \left(\frac{1-M^2}{\gamma M^2}\right) \tag{6}$$

where, f is known as the *Darcy friction factor*. For this equation, the M is the inlet Mach number and the outlet Mach number for $L = L_{max}$ is considered to be $M = 1$. Since it is expected that for microchannels f will differ from the ($64/Re$) value for a pipe obtained using the no-slip model, next f should be derived as a function of Kn using the first and second order velocity-slip models. To do this the geometry of the problem shown in Fig. 1 is considered again. For a constant area circular pipe with a radius R and assuming a fully developed, laminar flow, the continuity and momentum equation are reduced to the following:

$$\frac{1}{d}\frac{d}{dr}\left(r\frac{du}{dr}\right) = \frac{1}{\mu}\frac{dp}{dx} = const \tag{7}$$

This is solved by integrating twice and applying the appropriate boundary conditions. Even though the velocity at the centerline is not known, from physical considerations it is known that the velocity must be finite at $r = 0$, which is our first boundary condition. Now, the second boundary condition, the velocity at the wall must be applied. Here, the slip velocity at the wall will be introduced, once using the first order slip model and once using the second order model. So for the first order slip model the velocity at $r = R$ is:

$$u(R) = -\frac{2-\sigma_\upsilon}{\sigma_\upsilon}\lambda\left(\frac{\partial u}{\partial r}\right)_R \tag{8.1}$$

and for the second order slip model:

$$u(R) = -\frac{2-\sigma_\upsilon}{\sigma_\upsilon}\left[\lambda\left(\frac{\partial u}{\partial r}\right)_R + \frac{\lambda^2}{2}\left(\frac{\partial^2 u}{\partial r^2}\right)_R\right] \tag{8.2}$$

From these two conditions, the constants of integration can be found and the solutions for the velocity profiles for the two velocity-slip models are found. For the first order model the velocity is given by:

$$u(r) = \frac{1}{4\mu}\left(\frac{dp}{dx}\right)\left[r^2 - R^2\left(\frac{2-\sigma_\upsilon}{\sigma_\upsilon}\cdot 2Kn + 1\right)\right] \tag{9.1}$$

and for the second order model the velocity is:

$$u(r) = \frac{1}{4\mu}\left(\frac{dp}{dx}\right)\left[r^2 - R^2\left(\frac{2-\sigma_\upsilon}{\sigma_\upsilon}\cdot\left(2Kn + Kn^2\right) + 1\right)\right] \tag{9.2}$$

Once the velocity profiles are found a number of additional features of the flow can be derived from them. Also, the shear stress at the wall $\tau_w = -\mu\left(\frac{du}{dr}\right)_R$ can be derived from the velocity profiles, so when the first order slip and the second order slip models are used the shear stress at the wall is given for the first and second order model, respectively by:

$$\tau_w = \frac{4\mu\bar{V}}{R\left(\frac{2-\sigma_\upsilon}{\sigma_\upsilon}\cdot 4Kn + 1\right)}$$

and

$$\tau_w = \frac{4\mu\bar{V}}{R\left(\frac{2-\sigma_\upsilon}{\sigma_\upsilon}\cdot\left(4Kn + 2Kn^2\right) + 1\right)} \tag{10}$$

where, $\bar{V}$ is the mean velocity of the flow. Finally, the skin friction coefficient $C_f = \frac{2\tau_w}{\rho\bar{u}^2}$ can be obtained. The skin friction coefficient for the first order and second order slip models are given respectively by:

$$C_f = \frac{16}{\mathrm{Re}}\frac{1}{\left(\frac{2-\sigma_\upsilon}{\sigma_\upsilon}\cdot 4Kn + 1\right)}$$

and

$$C_f = \frac{16}{\mathrm{Re}} \frac{1}{\left(\frac{2-\sigma_v}{\sigma_v}\cdot\left(4Kn+2Kn^2\right)+1\right)} \quad (11)$$

As it can be seen from Eq. (11), for microchannels C_f (and consequently $f = 4C_f$) is a function of both *Re* and *Kn* numbers, so next the effect of changing *Kn* number will be investigated for the two slip models and compared to the no-slip model results.

RESULTS

After the above equations have been derived, they were used to plot the Fig. 2 to 11. The objective is to investigate the effect of change of the *Knudsen number (Kn)* on the flow characteristics derived previously for the range $0.001 \le Kn \le 0.1$. This is the range the Navier-Stokes equations with slip boundary conditions are considered in the literature to be applicable. For the purpose of this study the specific heat ratio γ is set to be $\gamma = 1.4$ (air).

Figure 2 and 3 show the effect changing the *Kn* number has on the shape of the velocity profiles for the fully developed laminar flow in a circular tube. As it can be seen by looking at these two figures, the velocity profiles for the two slip models is very similar in shape to the no-slip model velocity profile except for the amount of velocity-slip at the wall. Also, by comparing these two figures it is seen that increasing the *Kn* from 0.01 to 0.1 increases the slip at the pipe wall. Another thing which can be noticed from these two figures is that at *Kn = 0.01* the profiles of the two slip models practically overlap, while at *Kn = 0.1* they differ but only by a small amount. The amount of slip at the wall is as a function of *Kn* for the two velocity-slip models is summarized in the next figure, Fig. 4. Here it is seen that even though the two models deviate significantly from the zero value for the no-slip model, for the studied *Kn* number range, they don't deviate significantly from one another. So assuming that a difference between the no-slip model and the first order velocity-slip of 10% or more is significant enough to justify the use of the velocity-slip model, is can be seen that for $Kn \ge 0.017$ the first order slip model should be used instead of the no-slip model. The difference between the first and the second order slip models does not come even close to 10% for the range under considerations so the use of the second order model to find the velocity distribution is neither necessary nor practical.

The next two figures show the skin friction coefficient C_f for the two velocity-slip models. The first figure, Fig. 5, represents C_f, as a function of *Kn* number for different values of the tangential-momentum-accommodation coefficient σ_v and using the two velocity-slip models. The tangential-momentum-accommodation coefficient σ_v depends on the type of the fluid, the solid

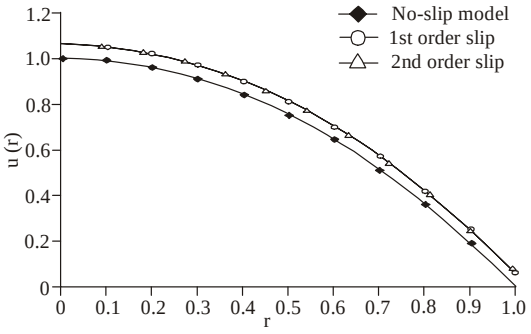

Fig. 2: Normalized velocity profiles for laminar flow inside circular pipe, using the no-slip, first order and second order slip models at *Kn = 0.01*

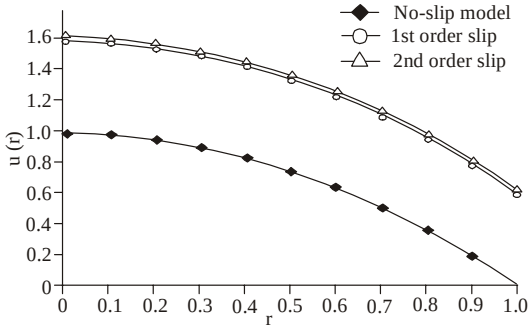

Fig. 3: Normalized velocity profiles for laminar flow inside circular pipe, using the no-slip, first order and second order slip models at *Kn = 0.1*

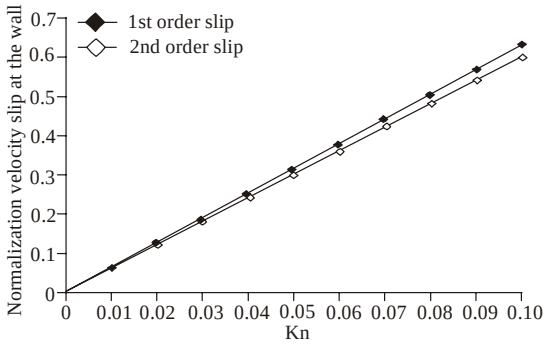

Fig. 4: Normalized velocity slip at the wall for the first order and second order slip models as a function of *Kn*

and on the surface finish. It has been experimentally determined to be between 0.2-0.8, the lower limit being for exceptionally smooth surfaces while the upper limit is typical for most practical surfaces. As it can be expected, the smaller σ_v value is, the lower the skin friction coefficient C_f is. From this figures it is also seen that increasing *Kn* decreases C_f. What is also noted from the figure is that for the range investigated, there is little difference between the results given by the first and the second order slip models. Since the difference between

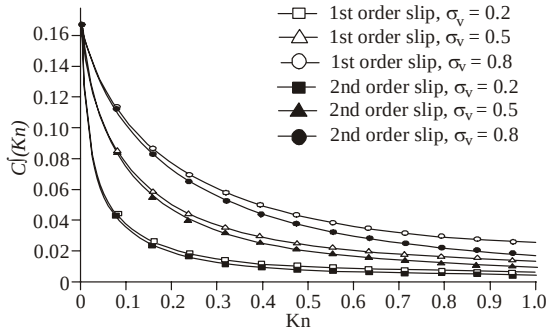

Fig. 5: Skin friction coefficient *Cf* as predicted by the first and second order slip models as a function of *Kn* for different values of the accommodation coefficient σ_v at *Re = 100*

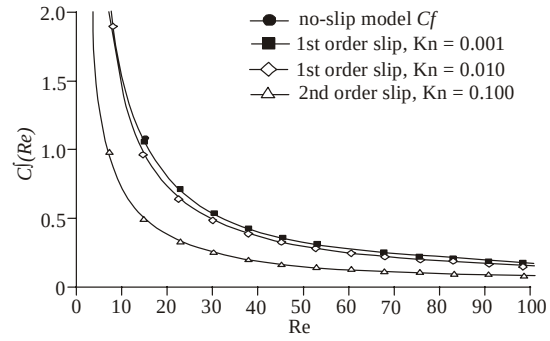

Fig. 6: Skin friction coefficient C_f for the no-slip and the first order slip models as a function of *Re* for different values of *Kn* and for $\sigma_v = 0.5$

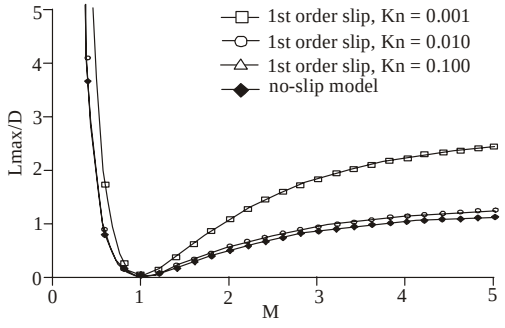

Fig. 7: Comparison between L_{max}/D *vs. M* for the first order slip model at different *Kn* with the no-slip model

the first order and the second ordr slip model seens to be negligible for the range under investigation, the next figure Fig. 6 shows the effect of *Re* on the C_f for the first order slip model only. It is plotted for different values of *Kn* and as it can be seen, the difference between the no-slip model and the first order slip model becomes apparent only for $Kn \geq 0.01$ and only for relatively low *Re* numbers. As the *Re* number increases this difference becomes smaller so for relatively small *Kn* and higher *Re* the difference becomes insignificant.

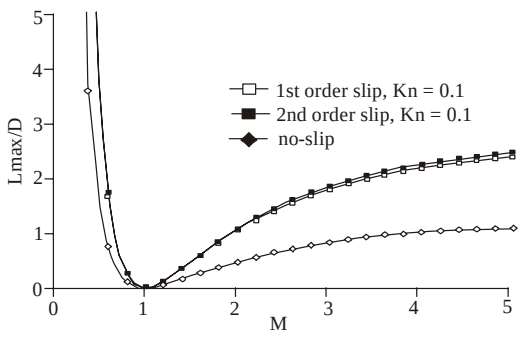

Fig. 8: Comparison between L_{max}/D *vs. M* for the no-slip, first order and second order slip models at *Kn = 0.1*

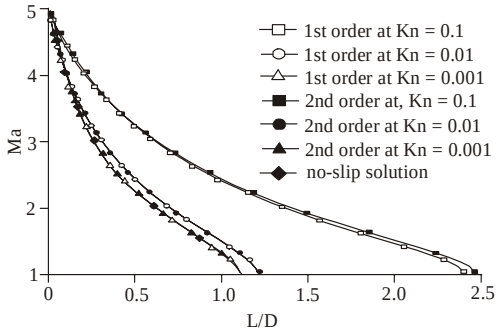

Fig. 9: Comparison between *M vs. L/D* for the no-slip, first order and second order slip models for supersonic flow regime

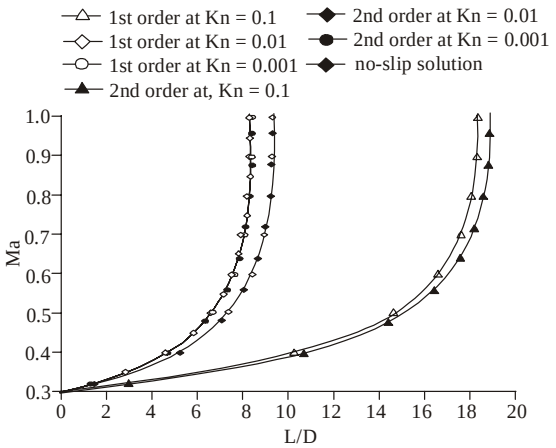

Fig. 10: Comparison between *M vs. L/D* for the no-slip, first order and second order slip models for subsonic flow regime

Meanwhile, Fig. 7 and 8, show how the change of the *Darcy friction coefficient f* ($fv = 4C_f$) with *Kn* number, affects the compressible fluid flow in circular tube. The L_{max}/D parameter is plotted against the *Mach number* (*M*) for the first order slip model along with the no-slip model. As it is seen from Fig. 7, the first order slip starts to deviate from the no-slip model for $Kn \geq 0.01$ and only for

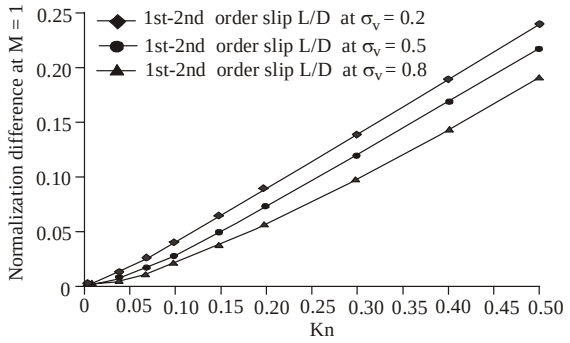

Fig. 11: Normalized difference between *L/D* for the first order and second order slip models as a function of *Kn* number

the supersonic flow regime. In the subsonic region, for $Kn \leq 0.01$, there is practically no difference between the no-slip and the first order slip models. In the next figure, Fig. 8, the second order slip model is plotted along with the first order slip and the no-slip models at $Kn = 0.1$. From this it is seen that although the two slip models deviate much from the no-slip model, they don't deviate from one another except for $M \geq 2$ and even then the difference between them is very small.

However, Fig. 9 and 10 are modified plots of *M* and *L/D* and show how a supersonic/subsonic fully-developed flow will behave as it enters a constant area duct and moves downstream. As a supersonic flow enters a microchannel, due to the friction with the wall it is decelerated along the path until it reaches $M = 1$ and Fig. 9 shows this velocity changes downstream. It is seen that increasing the *Kn* number will increase the *L/D* distance needed for the flow to reach $M = 1$. This should be expected because as it was seen above, increasing *Kn* decreases the friction coefficient *f*. For subsonic flow entering a pipe, due to the friction, the flow is accelerated along the way until it finally reaches $M = 1$ and Fig. 10 shows the velocity change along flow path. As for the supersonic flow, increasing the *Kn* number will increase the *L/D* distance needed for the flow to reach $M = 1$.

In the last figure, Fig. 11 the difference between the critical *L/D* values for the two velocity-slip models as a function of *Kn* for different values of The tangential-momentum-accommodation coefficient σ_v is summarized. What can be seen from looking at Fig. 9, 10 and 11 is that the difference between the first order slip and the second order slip models is very small compared to the difference between the first order slip and the no-slip model for the whole range of *Kn* number under investigation just as previously observed for the velocity profiles. So if the same criteria of a 10% difference are applied here also, these results would suggest that for an adiabatic compressible flow in circular microchannel, for $Kn \leq 0.01$ there is no need to apply any velocity-slip model as the no-slip model will give sufficiently accurate predictions, while for the range $0.01 \leq Kn \leq 0.1$, the first order velocity slip model should be applied and there is no necessity to use the second order velocity-slip model.

CONCLUSION

In the present study, the Fanno flow problem has been studied using both, first order and second order velocity-slip boundary conditions models and then compared to the no-slip boundary conditions solution. The aim of this is to observe the behavior of the flow predicted by the two slip models and to try and establish criteria for using the two velocity-slip models. The study concentrates on investigating the effect the change of *Kn* number has on the velocity profiles, magnitude of slip at the wall, skin friction coefficient C_f and the L_{max}/D factor characteristic of Fanno line. The Fanno flow is an ideal gas adiabatic flow in constant area duct with friction. For this case the circular pipe geometry has been chosen and all the flow characteristics have been derived for the first and second order velocity-slip models.

It is found that the velocity profile for the two velocity-slip models has generally the same shape as the no-slip model velocity profile but with a slip at the wall. This slip increases as the Kn increases and for $Kn \geq 0.01$ it becomes significant enough and the first order slip model should be used instead of the no-slip model. Also, the skin friction coefficient C_f is found to decrease as the *Kn* increases. Also the effect of the slip has on the compressible flow characteristics have been examined. It shows that as the *Kn* number increases, the friction coefficient *f* decreases. This reduction in friction leads to increase of the *L/D* parameter for both supersonic and subsonic flows with slip when compared to the no-slip solution.

Overall, it is concluded that for an adiabatic compressible flow in circular microchannel, for $Kn \leq 0.01$ there is no need to apply any velocity-slip model as the no-slip model will give sufficiently accurate predictions. As for the range $0.01 \leq Kn \leq 0.1$, the first order velocity slip model should be applied and that for this range, there is no necessity to use the second order velocity-slip model.

NOMENCLATURE

C_f = skin friction coefficient
D = *pipe diameter*
f = *Darcy friction coefficient*
Kn = *Knudsen number*
M = Mach number

p = *pressure*
R = pipe radius
Re = *Reynolds number*
r = radial coordinate
u = *axial velocity*
$\bar{v}$ = *mean velocity*
x = *axial coordinate*
γ = *specific heat ratio*
λ = *mean free path length*
μ = viscosity
ν = *kinematic viscosity*
ρ = *density*
σ_v = *tangential-momentum-accommodation coefficient*
τ_w = *shear stress at the wall*

ACKNOWLEDGMENT

The Authors extend their appreciation to the Deanship of Scientific Research at King Saud University for funding the work through the research group project No. RGP-VPP-036.

REFERENCES

Araki, T., M.S. Kim, H. Iwai and K. Suzuki, 2010. An experimental investigation of gaseous flow characteristics in micro channels. Micro Scale Therm. Eng., 6: 117-130.

Cai, C. and I.D. Boyd, 2007. Compressible gas flow inside a two-dimensional uniform micro channel. J. Therm. Heat Trans., 21(3).

Celata, G.P., M. Cumo, S.J. McPhail, L. Tesfagabir and G. Zummo, 2007. Experimental study on compressible flow in micro tubes. Int. J. Heat Fluid Flow, 28: 28-36.

Choi, S.B., R.F. Barron and R.O. Warrington, 1991. Fluid flow and heat transfer in micro tubes. Micromech. Sensors Actuators Syst., 32: 123-134.

Choquette, S.F., M. Faghri, E.J. Kenyon and B. Sunden, 1996. Compressible fluid flow in micron-sized channels. Nat. Heat Transfer Conf., 5: 25-32.

Chuang, R., H.F. Cruden and B.A.M. Meyyappan, 2003. Modeling gas flow through micro channels and nanopores. J. Appl. Phys., 93(8): 4870-4879.

Colin, S., P. Lalonde and R. Caen, 2010. Validation of a second-order slip flow model in rectangular micro channels. Heat Transfer Eng., 25: 23-30.

Demsis, A., B. Verma, S.V. Prabhu and A. Agrawal, 2009. Experimental determination of heat transfer coefficient in the slip regime and its anomalously low value. Phys. Rev. E, 80: 016311-8.

Gad-el-Hak, M., 1999. The fluid mechanics of micro devices-the freeman scholar lecture. J. Fluid Eng., 121: 5-33.

Gad-el-Hak, M., 2002. Flow Physics in Microdevices. The Handbook of MEMS, CRC Press, Boca Raton, Florida.

Gamrat, G., M. Favre-Marinet, S. Le Person, R. Bavière and F. Ayela, 2008. An experimental study and modelling of roughness effects on laminar flow in microchannels. J. Fluid Mech., 594: 399-423.

Harley, J.C., Y. Huang, H. Bau and J.N. Zemel, 1995. Gas flows in micro-channels. J. Fluid Mech., 284: 257-274.

Ho, C. and Y. Tai, 1998. Micro-Electro-Mechanical Systems (MEMS) and fluid flows. Ann. Rev. Fluid Mech., 30: 579-612.

Hsieh, S., H. Tsai, C.Y. Lin, C.F. Huang, C.M. Chien, 2004. Gas flow in a long micro channel. Int. J. Heat Mass Transfer, 47: 3877-3887.

John, J.E., 1984. Gas Dynamics. 2nd Edn., Allyn & Bacon, Boston.

Matsuda, Y., T. Uchida, S. Suzuki, R. Misaki, H. Yamaguchi and T. Niimi, 2011. Pressure-sensitive molecular film for investigation of micro gas flows. Microfluid. Nanofluid., 10: 165-171.

Karniadakis, G. and A. Beskok, 2002. Micro Flows Fundamentals and Simulation. Springer, New York.

Kashid, M., A. Renken and L. Kiwi-Minsker, 2011. Mixing efficiency and energy consumption for five generic microchannel designs. Chem. Eng. J., 167: 436-443.

Kim, D.K. and S.J. Kim, 2007. Closed-form correlations for thermal optimization of micro channels. Int. J. Heat Mass Transfer, 50: 5318-5322.

Kim, J.H., S. Baek, S. Jeong and J. Jung, 2010. Hydraulic performance of a microchannel PCHE. Appl. Therm. Eng., 30: 2157-2162.

Koochesfahani, M.M. and D. Nocera, 2007. Molecular Tagging Velocimetry. In: C.T.J. Foss and A. Yarin (Eds.), Handbook of Experimental Fluid Dynamics. Springer-Verlag, Ch: 5.4.

Marino, L., 2009. Experiments on rarefied gas flows through tubes. Microfluid. Nanofluid. 6: 109-119.

Matsuda, Y., H. Mori, Y. Sakazaki, T. Uchida, S. Suzuki, H. Yamaguchi and T. Niimi, 2009. Extension and characterization of pressure-sensitive molecular film. Exp. Fluids, 47: 1025-1032.

Morini, G.L., M. Lorenzini and S. Salvigni, 2006. Friction characteristics of compressible gas flows in microtubes. Exp. Therm. Fluid Sci., 30: 733-744.

Morini, G.L., M. Lorenzini, S. Colin and S. Geoffroy, 2007. Experimental analysis of pressure drop and laminar to turbulent transition for gas flows in smooth micro tubes. Heat Transfer Eng., 28: 670-679.

Morini, G.L., Y. Yang, H. Chalabi and M. Lorenzini, 2011. A critical review of the measurement techniques for the analysis of gas micro flows through micro channels. Exp. Therm. Fluid Sci., 35(6): 849-865.

Petropoulos, A., G. Kaltsas, D. Randjelovic and E. Gogolides, 2010. Study of flow and pressure field in microchannels with various cross-section areas. Micro. Eng., 87: 827-829.

Pitakarnnop, J., S. Varoutis, D. Valougeorgis, S. Geoffroy, L. Baldas and S. Colin, 2010. A novel experimental setup for gas microflows. Microfluid. Nanofluid., 8: 57-72.

White, F.M., 1991. Viscous Fluid Flow. 2nd Edn, McGraw-Hill, Inc., New York, pp: 116-118.

Wu, H.Y. and P. Cheng, 2003. Friction factors in smooth trapezoidal silicon microchannels with different aspect ratios. Int. J. Heat nd Mass Transfer, 46: 2519-2525.

Yang, Y., G.L. Morini and M. Lorenzini, 2010. Experimental analysis of gas micro-convection through commercial microtubes. Proceeding of 2nd European Conference on Microfluidics (uFlu10), Toulouse (F).